The Astrophysical Journal, 787:162 (9pp), 2014 June 1 doi:10.1088/0004-637X/787/2/162

EXPLORING THE ORIGIN OF LITHIUM, CARBON, STRONTIUM, AND BARIUM WITH FOUR NEW ULTRA METAL-POOR STARS*

T. Hansen[1], C. J. Hansen[1], N. Christlieb[1], D. Yong[2], M. S. Bessell[2], A. E. García Pérez[3], T. C. Beers[4,5], V. M. Placco[6], A. Frebel[7], J. E. Norris[2], and M. Asplund[2]

[1] Landessternwarte, ZAH, Königstuhl 12, D-69117 Heidelberg, Germany; thansen@lsw.uni-heidelberg.de, cjhansen@lsw.uni-heidelberg.de, nchristlieb@lsw.uni-heidelberg.de

[2] Research School of Astronomy and Astrophysics, The Australian National University, Weston, ACT 2611, Australia; yong@mso.anu.edu.au, bessell@mso.anu.edu.au, john.norris@anu.edu.au, martin.asplund@anu.edu.au

[3] Department of Astronomy, University of Virginia, Charlottesville, VA 22904-4325, USA; aeg4x@virginia.edu

[4] National Optical Astronomy Observatory, Tucson, AZ 85719, USA; beers@noao.edu

[5] JINA: The Joint Institute for Nuclear Astrophysics, 225 Nieuwland Science Hall, Department of Physics, University of Notre Dame, Notre Dame, IN 46556-5670, USA

[6] Gemini Observatory, Hilo, HI 96720, USA; vplacco@gemini.edu

[7] Department of Physics, Massachusetts Institute of Technology, Cambridge, MA 02139, USA; afrebel@mit.edu

Received 2013 November 14; accepted 2014 April 8; published 2014 May 15

ABSTRACT

We present an elemental abundance analysis for four newly discovered ultra metal-poor stars from the Hamburg/ESO survey, with [Fe/H] $\leqslant -4$. Based on high-resolution, high signal-to-noise spectra, we derive abundances for 17 elements in the range from Li to Ba. Three of the four stars exhibit moderate to large overabundances of carbon, but have no enhancements in their neutron-capture elements. The most metal-poor star in the sample, HE 0233−0343 ([Fe/H] = −4.68), is a subgiant with a carbon enhancement of [C/Fe] = +3.5, slightly above the carbon-enhancement plateau suggested by Spite et al. No carbon is detected in the spectrum of the fourth star, but the quality of its spectrum only allows for the determination of an upper limit on the carbon abundance ratio of [C/Fe] < +1.7. We detect lithium in the spectra of two of the carbon-enhanced stars, including HE 0233−0343. Both stars with Li detections are Li-depleted, with respect to the Li plateau for metal-poor dwarfs found by Spite & Spite. This suggests that whatever site(s) produced C either do not completely destroy lithium, or that Li has been astrated by early-generation stars and mixed with primordial Li in the gas that formed the stars observed at present. The derived abundances for the α elements and iron-peak elements of the four stars are similar to those found in previous large samples of extremely and ultra metal-poor stars. Finally, a large spread is found in the abundances of Sr and Ba for these stars, possibly influenced by enrichment from fast rotating stars in the early universe.

Key words: early universe – Galaxy: formation – Galaxy: halo – nuclear reactions, nucleosynthesis, abundances – stars: abundances

Online-only material: color figures

1. INTRODUCTION

The stellar atmospheres of the first generations of low-mass ($M \leqslant 0.8\,M_{\odot}$) stars are expected to retain, to a large extent, detailed information on the chemical composition of the nearly pristine gas of the interstellar medium (ISM) at the time and place of their birth. Detailed abundance analyses of metal-poor stars thus enable studies of the formation and evolution of the elements in the early Galaxy. At these early times, the two light elements carbon and lithium play a major role in cosmological studies, as well as in our understanding of early star formation. In addition, the production site(s) of the elements beyond the iron peak remains a major unanswered question.

Recent studies, such as Carollo et al. (2012), Lee et al. (2013), and Norris et al. (2013b) confirm that carbon-enhanced metal-poor (CEMP) stars[8] constitute a large fraction of the most metal-poor stars known and that the fraction of CEMP stars increases dramatically with decreasing metallicity, accounting for ∼40% of all stars with [Fe/H] $\leqslant -3.5$. In fact, four of the five stars previously known with [Fe/H] < -4.5 are confirmed CEMP stars (Christlieb et al. 2002; Frebel et al. 2005; Norris et al. 2007; Caffau et al. 2011; Keller et al. 2014). In this paper, we add another confirmed CEMP star with [Fe/H] < -4.5, as described below.

Beers & Christlieb (2005) specify a nomenclature that identifies a number of subclasses for CEMP stars. The CEMP-*s* stars exhibit overabundances of elements predominantly produced by the so-called slow neutron-capture process, or *s* process, such as barium. These stars are the most commonly observed subclass of CEMP stars; around 80% of CEMP stars exhibit *s*-process element enhancements (Aoki et al. 2007), including both the CEMP-*s* and CEMP-*r*/*s* subclass (stars that, in addition to exhibiting *s*-process element enhancement, are also enhanced in elements predominantly produced in the rapid neutron-capture process, or *r* process, such as europium). The favored scenario for the production of CEMP-*s* (and CEMP-*r*/*s*) stars is mass transfer of carbon- and *s*-process-enhanced material from the envelope of an asymptotic giant branch (AGB) star to its (presently observed) binary companion (e.g., Herwig 2005; Sneden et al. 2008). Observational evidence now exists to suggest that the CEMP-*r*/*s* stars (and other *r*-process-element-rich stars) were enhanced in *r*-process elements in their natal gas clouds by previous generations of supernovae (SNe), and did

* Based on observations made with the European Southern Observatory (ESO) Telescopes.

[8] Originally defined by Beers & Christlieb (2005) as metal-poor ([Fe/H] $\leqslant -1.0$) stars with [C/Fe] $\geqslant +1.0$; a level of carbon enrichment [C/Fe] $\geqslant +0.7$ is used in most contemporary work.

not require a contribution of *r*-process elements from a binary companion (see Hansen et al. 2011).

The CEMP-no subclass includes CEMP stars that exhibit no enhancements in their neutron-capture elements. It has been shown that at extremely low metallicity, [Fe/H] < -3.0, the CEMP-no stars are the dominant subclass (Aoki 2010; Norris et al. 2013b). Different progenitors have been suggested for the CEMP-no stars, such as pollution by faint SNe that experienced extensive mixing and fallback during their explosions (Umeda & Nomoto 2003, 2005; Tominaga et al. 2007, 2013; Ito et al. 2009, 2013; Nomoto et al. 2013),[9] winds from massive, rapidly rotating, mega metal-poor ([Fe/H] < -6.0) stars, sometimes referred to as "spinstars" (Hirschi et al. 2006; Meynet et al. 2006; Hirschi 2007; Meynet et al. 2010; Cescutti et al. 2013), or mass transfer from an AGB star companion (Suda et al. 2004; Masseron et al. 2010). This latter explanation encounters difficulties, however, when confronted with results from recent radial-velocity monitoring programs.

Radial-velocity data support the expected differences in the binary nature of CEMP-*s* (CEMP-*r*/*s*) and CEMP-no stars. Lucatello et al. (2005) argued that multiple-epoch observations of CEMP-*s* stars are consistent with essentially all CEMP-*s* (CEMP-*r*/*s*) stars being members of binary systems. Although more data are desired for CEMP-no stars, Hansen et al. (2013) report that the fraction of binaries among stars of this class is no higher than expected for random samples of very metal-poor giants. Norris et al. (2013b) reach similar conclusions for their limited radial-velocity data for a number of CEMP-no stars.

The measured Li abundances of CEMP stars do not show an obvious correlation with C at the lowest metallicities, but do exhibit a general downward trend with declining [Fe/H]. Masseron et al. (2012) considered the CEMP stars with measured Li reported in the literature and added 13 new stars to the list; they highlight the large spread in the measured Li abundances for CEMP stars. In addition to the production of Li during big bang nucleosynthesis, Li can also be produced via the Cameron–Fowler mechanism in AGB stars if ^{7}Be, created at the bottom of the convective envelope, captures an electron (Sackmann & Boothroyd 1992). If CEMP stars are the result of mass transfer from an AGB companion, then the Li abundances in CEMP stars will reflect a combination of (1) Galactic chemical evolution and (2) Li production/destruction in the AGB companion. Additional data are necessary to explore and test this hypothesis in more detail. It should also be recalled that Piau et al. (2006) argued that primordial Li could be astrated by first-generation stars, objects similar in nature to the massive-star progenitors suggested for CEMP-no stars. In this view, the fact that Li abundances for CEMP-no stars are always below the level of the Spite Li plateau (see, e.g., Masseron et al. 2012) can be understood as the result of various degrees of local mixing between Li-astrated material ejected from first-generation stars and the surrounding gas having the primordial level of Li.

Most elements beyond the iron peak are produced by neutron capture, either in the *s* process or the *r* process (e.g., Burbidge et al. 1957; Sneden et al. 2008). The neutron-capture elements strontium and barium are those that are most easily measured in low-metallicity stars. At solar metallicity, these elements are produced in the main *s* process in AGB stars (Busso et al. 1999; Käppeler et al. 2011), but at low metallicity, AGB stars may not have had time to sufficiently enrich the ISM. Hence, the Sr and Ba abundances observed in low-metallicity stars are presumably produced via the main *r* process, most likely occurring in the final stages of the life of massive stars (Truran 1981; Thielemann et al. 2011), or in the weak *s* process suggested to occur in spinstars (Pignatari et al. 2008; Cescutti et al. 2013).

More studies of the lowest metallicity stars are required to gain a deeper understanding of the nucleosynthesis processes taking place in the early universe, for both the light and heavy elements, since at present fewer than 10 stars with [Fe/H] $\leqslant -4.2$ have been analyzed. This paper presents four newly discovered ultra metal-poor (UMP) stars ([Fe/H] < -4.0), three of which are enhanced in carbon but not in neutron-capture elements, and are hence classified as CEMP-no stars. We also detect lithium in the spectra of two of the stars, one of these being the second most metal-poor star with detected Li known to date.

2. OBSERVATIONS AND DATA ANALYSIS

The four stars presented in this paper are part of a larger sample of metal-poor candidates selected from the Hamburg/ESO survey, followed up with medium-resolution spectroscopy on a variety of 2–4 m class telescopes, then observed at high spectral resolution with Very Large Telescope (VLT)/UVES (Dekker et al. 2000). The complete sample will be presented in Paper II of this series, along with a detailed description of the observations, data reduction procedure, parameter determination, and abundance analysis. Here, only the key points of the techniques employed are listed.

Figure 1 shows the medium-resolution spectra of the program stars. It is possible to see features such as the Ca II K line, H_β, H_γ, and H_δ, as well as the CH and CN molecular carbon bands for HE 1310−0536. Both the Southern Astrophysical Research (SOAR) 4.1 m and KPNO/Mayall 4 m data have a wavelength coverage of 3550–5500 Å, with a resolving power of $R \sim 1500$ and signal-to-noise ratios of S/N $\sim$ 30 pixel^{-1} at 4000 Å. For the ESO 3.6 m data, the resolving power and signal-to-noise were similar to the SOAR 4.1 m and Mayall 4 m data, but the wavelength range is narrower, covering the interval 3700–5100 Å.

Medium-resolution spectra obtained with the Wide Field Spectrograph (Dopita et al. 2007) on the Australian National University 2.3 m Telescope at Siding Spring Observatory were used for the temperature determination.

The high-resolution data was obtained during the nights of 2005 November 17 and 20, and 2006 April 17. The data cover a wavelength range from 3100 Å to 9500 Å, with a resolving power of $R \sim 45{,}000$. The spectra were reduced using the UVES reduction pipeline, version 4.9.8. Radial-velocity shifts, co-addition of the spectra, and continuum normalization were all performed using IRAF.[10] The average S/N of the reduced spectra is S/N $\sim$ 10, $\sim$30, and $\sim$55 pixel^{-1} at 3400 Å, 4000 Å, and 6700 Å, respectively.

2.1. Stellar Parameters

The stellar atmospheric parameters were determined by standard techniques, generally following the steps outlined in Yong et al. (2013). Effective temperatures were determined by fitting the spectrophotometric observations with model atmosphere

[9] This model well-reproduces the observed elemental-abundance pattern of the CEMP-no star BD+44°493, the ninth-magnitude, [Fe/H] = −3.8 star (with [C/Fe] = +1.3, [N/Fe] = +0.3, [O/Fe] = +1.6) discussed by Ito et al. (2009, 2013).

[10] IRAF is distributed by the National Astronomy Observatory, Inc., under cooperative agreement with the National Science Foundation.

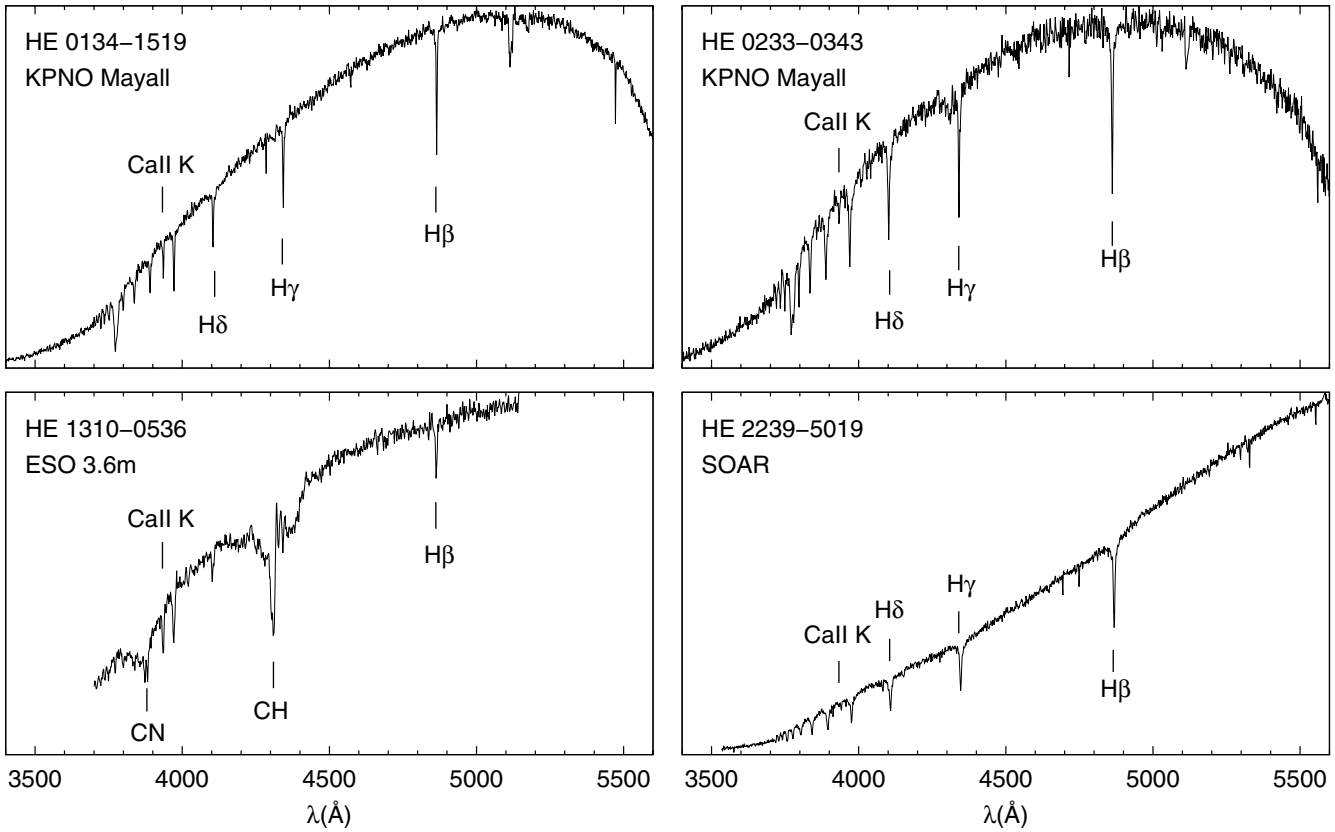

Figure 1. Medium-resolution spectra of our four program stars. The locations of the Ca II K line, H_β, H_γ, and H_δ lines are shown. For HE 1310−0536, the CH and CN molecular carbon bands are clearly visible.

fluxes (Bessell 2007; Norris et al. 2013a). LTE model atmosphere fluxes from the MARCS grid (Gustafsson et al. 2008), with $[\alpha/\mathrm{Fe}] = +0.4$, were used for the model fitting. Estimates of surface gravity were determined from the Y^2 isochrones (Demarque et al. 2004), assuming an age of 10 Gyr and an α-element enhancement of $[\alpha/\mathrm{Fe}] = +0.3$. These isochrones only extend down to $[\mathrm{Fe/H}] = -3.5$; therefore, a linear extrapolation down to $[\mathrm{Fe/H}] = -4.7$ has been used to obtain the surface-gravity estimates for our four stars. The average difference between the listed surface gravities, where the actual [Fe/H] values have been used, and the surface gravity obtained using the $[\mathrm{Fe/H}] = -3.5$ isochrone, is rather small (on the order of 0.07 dex). Metallicities were determined from equivalent-width measurements of the Fe I lines. Non-LTE (NLTE) effects might be present in the Fe I lines, which can affect the derived metallicity (Lind et al. 2012), but no Fe II lines were detected in any of the four program stars. The measured Fe abundance may also be subject to uncertainties from three-dimensional (3D) effects. Collet et al. (2006) report a 3D correction of ~ -0.2 dex for the Fe abundance for two of the most metal-poor stars known (HE 0107−5240 and HE 1327−2326), both of which have temperatures and gravities that are comparable, within the combined error bars, to those of the stars presented in this paper. A better basis for comparison, at the same metallicity as our program stars, is clearly desirable. Bergemann et al. (2012) found, however, that departures from LTE will likely partly compensate such 3D LTE effects, leaving a smaller net effect. Our stars have several Fe I lines in common with the study of Bergemann et al. (2012). A full 3D NLTE study is clearly warranted, but beyond the scope of the present study.

The microturbulent velocity was computed in the usual way, by forcing the abundances from Fe I lines to show no trend with reduced equivalent width, $\log(W_\lambda/\lambda)$. For HE 0233−0343, too few Fe I lines were present to determine the microturbulent velocity in this way, so a fixed valued of $\xi = 2$ km s^{-1} was used for this star.

For the warmer stars, HE 0233−0343 and HE 2239−5019, two possible solutions for the surface gravity were found. Several tests were made to settle on the listed values, both consistent with subgiant, rather than dwarf, classifications. This aspect will be explored further in Paper II of this series. The final stellar parameters and their associated uncertainties are listed in Table 1.

2.2. Abundance Analysis

The abundance analysis has been carried out by synthesizing individual spectral lines with the 2011 version of MOOG (Sneden 1973), which includes a proper treatment of continuum scattering (Sobeck et al. 2011). A set of α-enhanced ATLAS9 models (Castelli & Kurucz 2003) have been used, along with interpolation software tested in Allende Prieto et al. (2004), which produces models with the required stellar parameters (e.g., Reddy et al. 2003; Allende Prieto et al. 2004). For HE 0233−0343, the metallicity in the model atmosphere was $[m/\mathrm{H}] = -4.5$, which differs by 0.18 dex from the metallicity of the star. This difference is within the uncertainty of the derived [Fe/H] of the star and given the small difference, we expect no change in any of the abundances when using a model with $[m/\mathrm{H}] = -4.7$.

The *Gaia*/ESO line list version 3 has been used (U. Heiter et al., in preparation). Atomic data from VALD (Kupka et al. 2000) were adopted for lines not included in that line list. Hyperfine splitting was taken into account for lines of Sc,

Table 1
Stellar Parameters and Derived Abundances

	HE 0134−1519	HE 0233−0343	HE 1310−0536	HE 2239−5019
R.A.	01 37 05.4	02 36 29.7	13 13 31.2	22 42 26.9
Decl.	−15 04 24	−03 30 06	−05 52 13	−50 04 01
V[a]	14.47	15.43	14.35	15.85
$B-V$[a]	0.50	0.34	0.71	0.39
$J-K$[a]	0.43	0.30	0.64	0.40
Radial velocity (km s^{-1})	244	64	113	370
Parameters				
$T_{\rm eff}$ (±100 K)	5500	6100	5000	6100
log g (±0.3 dex)	3.2	3.4	1.9	3.5
[Fe/H] (±0.2 dex)	−4.0	−4.7	−4.2	−4.2
ξ (±0.3 km s^{-1})	1.5	2.0	2.2	1.8
Abundances				
A(Li)	1.27 (0.19)	1.77 (0.18)	<0.80 ···	<1.70 ···
[Fe/H]	−3.98 (0.30)	−4.68 (0.30)	−4.15 (0.30)	−4.15 (0.30)
[C/Fe]	+1.00 (0.26)	+3.48 (0.24)	+2.36 (0.23)	<+1.70 ···
[N/Fe]	<+1.00 ···	<+2.80 ···	+3.20 (0.37)	<+2.70 ···
[Na/Fe]	−0.24 (0.15)	<+0.50 ···	+0.19 (0.14)	<−0.30 ···
[Mg/Fe]	+0.25 (0.14)	+0.59 (0.15)	+0.42 (0.16)	+0.45 (0.15)
[Al/Fe]	−0.38 (0.20)	<+0.03 ···	−0.39 (0.21)	−0.57 (0.21)
[Si/Fe]	+0.05 (0.16)	+0.37 (0.15)	<+0.25 ···	+0.06 (0.15)
[Ca/Fe]	+0.10 (0.13)	+0.34 (0.15)	0.00 (0.20)	+0.23 (0.15)
[Sc/Fe]	−0.10 (0.18)	<+0.20 ···	−0.23 (0.16)	+0.26 (0.16)
[Ti/Fe]	+0.11 (0.21)	+0.18 (0.17)	+0.35 (0.18)	+0.37 (0.17)
[Cr/Fe]	−0.22 (0.18)	<+0.50 ···	−0.49 (0.26)	0.00 (0.17)
[Mn/Fe]	−1.19 (0.19)	<−0.10 ···	−1.40 (0.20)	<−0.60 ···
[Co/Fe]	+0.25 (0.18)	<+1.60 ···	+0.10 (0.16)	<+0.70 ···
[Ni/Fe]	+0.19 (0.19)	<+0.90 ···	−0.12 (0.20)	+0.24 (0.17)
[Sr/Fe]	−0.30 (0.19)	+0.32 (0.19)	−1.08 (0.14)	<−0.60 ···
[Ba/Fe]	<−0.50 ···	<+0.80 ···	−0.50 (0.15)	<0.00 ···

Note. [a] Beers et al. (2007).

Mn, and Co, using the data from Kurucz (1995). For Ba and Li, both hyperfine splitting and isotope shifts are present, and data from McWilliam (1998) and Asplund et al. (2006) were included, respectively. The molecular information for CH, CN, and NH was kindly provided from T. Masseron (2014, private communication).

The derived elemental abundances, along with propagated uncertainties arising from the effects of uncertain stellar parameters, continuum placement, and line information, are listed in Table 1. The adopted solar abundances are from Asplund et al. (2009). All listed abundances are derived under one-dimensional (1D) and LTE assumptions. NLTE effects will be explored in Paper II.

3. RESULTS

3.1. Radial Velocity

Two of the stars listed in Table 1, HE 0134−1519 and HE 2239−5019, exhibit quite high radial velocities, 244 km s^{-1} and 370 km s^{-1}, respectively. The uncertainty of the listed radial velocities is on the order of ∼1 km s^{-1}. Such high velocities may suggest membership in the proposed outer-halo population of the Milky Way (Carollo et al. 2007, 2010; Beers et al. 2012). A kinematic analysis of the full space motions of our complete program sample, including the four stars reported on here, will be presented in Paper II of this series. In this context, it is interesting that Carollo et al. (2014) present tentative evidence that the CEMP-*s* and CEMP-no stars may well be associated with progenitors that belong, in different proportion, to the suggested inner- and outer-halo populations of the Milky Way.

3.2. Elemental Abundances

Our analysis has produced abundance estimates, or upper limits, for 17 elements—Li, C, N, Na, Mg, Al, Si, Ca, Sc, Ti, Cr, Mn, Fe, Co, Ni, Sr, and Ba. We describe these analyses in detail in the subsections below.

3.2.1. Lithium

We derived lithium abundances from synthesis of the Li I 6707.8 Å doublet. Lithium is detected for two of our program stars–HE 0134−1519, with A(Li) = 1.27,[11] and HE 0233−0343, with A(Li) = 1.77. Figure 2 shows the spectral region around the Li line for two of our stars (top: HE 0134−1519, and bottom: HE 0233−0343), together with three synthetic spectra computed with A(Li) = 1.46, 1.27, and 1.08, respectively, for HE 0134−1519, and A(Li) = 1.95, 1.77, and 1.59, respectively, for HE 0233−0343. HE 0233−0343 is the second most metal-poor star with a detected lithium line, as lithium was also detected in the most metal-poor star known, SMSS J031300.36−670839.3 with [Fe/H] < −7, recently discovered by Keller et al. (2014) (A(Li) = 0.7). Li is not detected for the two remaining program stars; we computed upper limits of A(Li) < 0.8 and A(Li) < 1.70 for HE 1310−0536 and HE 2239−5019, respectively. The very low upper limit detected in HE 1310−0536 is expected, as

[11] A(Li) is defined in the usual manner, $A(\mathrm{Li}) = \log(N(\mathrm{Li})/N(\mathrm{H})) + 12$.

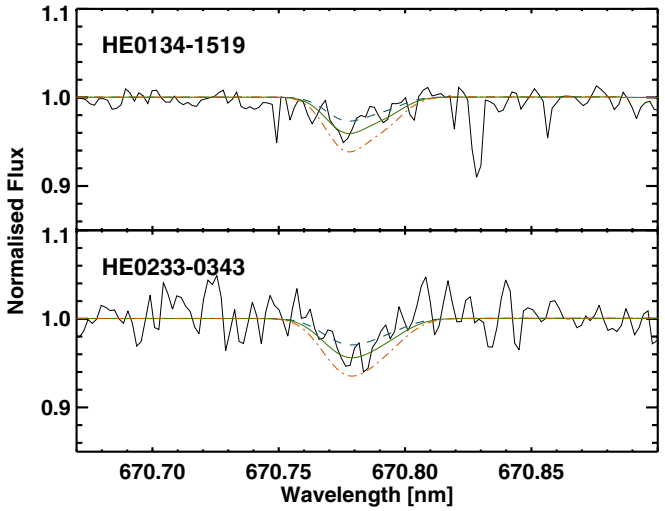

Figure 2. Li line fit for HE 0134−1519 (top) A(Li) = 1.46, 1.27, and 1.08 (blue dashed line, solid green line, and red dot–dashed line, respectively) and HE 0233−0343 (bottom) A(Li) = 1.95, 1.77, and 1.59 (blue dashed line, solid green line, and red dot–dashed line, respectively). The blue dashed and red dot–dashed lines correspond to $A(\mathrm{Li}) \pm \sigma(\mathrm{Li})$, respectively, as listed in Table 1.

(A color version of this figure is available in the online journal.)

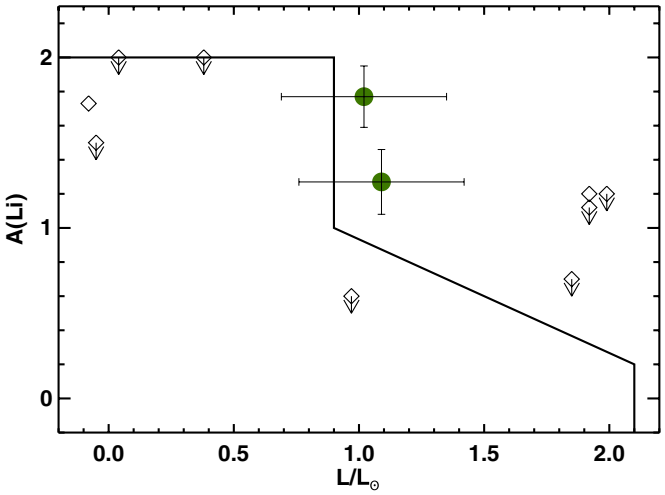

Figure 3. LTE lithium abundances, A(Li), as a function of luminosity, for HE 0134−1519 and HE 0233−0343 (green circles), along with the CEMP-no stars of Masseron et al. (2012) (black diamonds). Upper limits are indicated by arrows. The solid line indicates the division between Li-normal (above) and Li-depleted (below) stars.

(A color version of this figure is available in the online journal.)

this star is sufficiently evolved that it has undergone first dredge up. Its convective zone likely extends down to layers in the atmosphere where lithium has been destroyed by nuclear burning.

Figure 3 displays the Li abundance for our two CEMP-no stars with Li detections, as a function of their luminosity, following Figure 16 of Masseron et al. (2012). Luminosities have been determined in the same way as in Masseron et al. (2012), assuming $M = 0.8\ M_{\odot}$. For comparison, we also plot the CEMP-no stars of their sample. The solid line marks the division between Li-normal (above) and Li-depleted (below) stars. The line is computed from the Li abundance of non-CEMP stars with luminosities in the range $-0.2 < \log(L/L_{\odot}) < 2.1$. The line follows the Spite Li plateau for dwarf stars, then exhibits a linear decline in the Li abundances of giants, where the Li is expected to be gradually depleted due to convective burning episodes (see

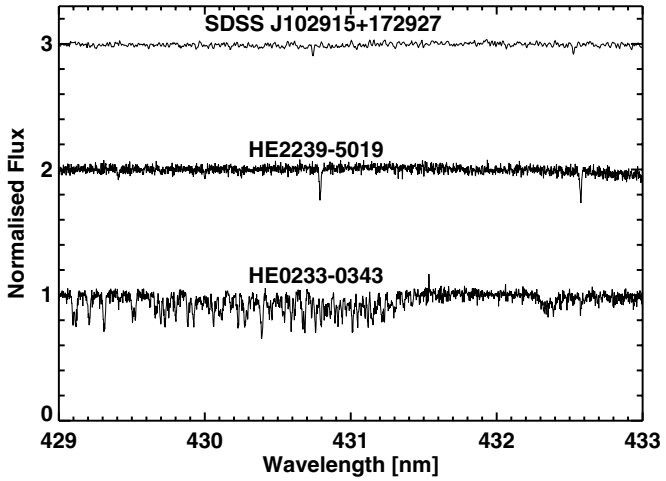

Figure 4. Spectral range including the CH G band in the spectra of SDSS J102915+172927 (top), HE 2239−5019 (middle), and HE 0233−0343 (bottom). The carbon lines are clearly seen in the spectrum of HE 0233−0343, but are absent in the other two spectra.

Masseron et al. 2012 for details). Stars outside the above range in luminosity are expected to have destroyed all their Li. Note that HE 1310−0536, with $\log(L/L_{\odot}) = 2.11$, falls outside that range. Our two Li detections both lie above the Li-normal line, but with lithium abundances below the Spite plateau. Hence, Li has been depleted in these stars, consistent with the result found by Masseron et al. (2012), that the CEMP-no class only contains Li-depleted stars, even at these low metallicities.

3.2.2. Carbon

Three of our four program stars, HE 0134−1519, HE 0233−0343, and HE 1310−0536, are carbon enhanced, with [C/Fe] $\geqslant$ +0.7. They exhibit no enhancements in their neutron-capture elements ([Ba/Fe] $\leqslant$ 0.0; Beers & Christlieb 2005), and are considered CEMP-no stars. Technically, the status of HE 0233−0343 cannot be confirmed, as only an upper limit for the Ba abundance of [Ba/Fe] < +0.8 is found. Considering that the great majority of CEMP stars with [Fe/H] < −3 are CEMP-no stars (Aoki 2010), and the fact that there are no known CEMP-s stars with [Fe/H] < −3.5, there is a high likelihood that HE 0233−0343 also belongs to the CEMP-no class. The last of the four stars, HE 2239−5019, shows no clear carbon enhancement; we compute an upper limit of [C/Fe] < +1.7 for this star. With no carbon detected, this star is a potential candidate to be in the same class as SDSS J102915+172927, the only star with [Fe/H] < −4.5 found not to be carbon enhanced (Caffau et al. 2011).

Figure 4 shows the spectral range including the CH G band for SDSS J102915+172927, HE 2239−5019, and HE 0233−0343. HE 0233−0343 has similar stellar parameters as HE 2239−5019, but it is more iron poor and carbon enhanced. Similar to SDSS J102915+172927, no CH features are visible in HE 2239−5019. However, the noise level in the spectrum of HE 2239−5019 is quite high, resulting in a high derived upper limit on the carbon abundance, so it cannot be ruled out as being a CEMP star.

Since three out of the four stars are carbon enhanced, the oxygen and nitrogen abundances are also of interest. Nitrogen was detected in only one star, HE 1310−0536, where the abundance listed in Table 1 is derived from synthesis of the CN band at 3883 Å. For the remaining three stars, upper limits are derived from synthesis of the NH band at 3360 Å. Previous

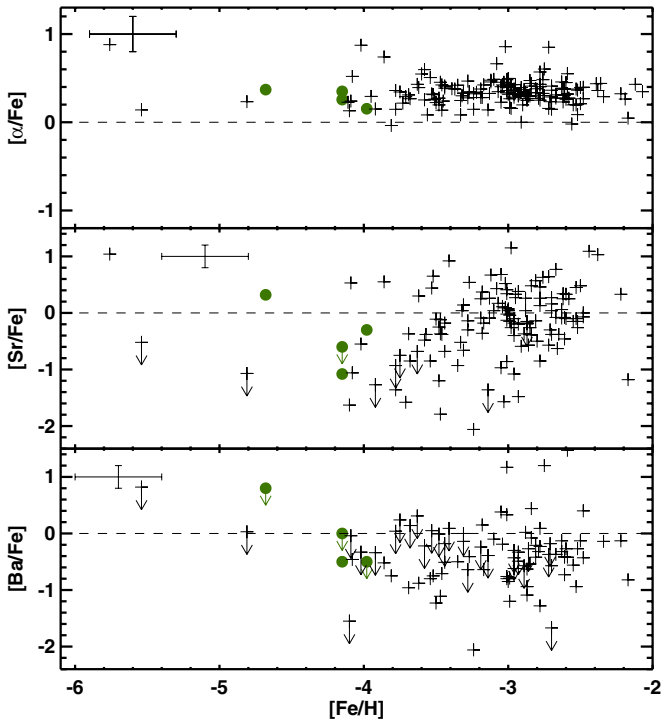

Figure 5. Mean [α/Fe] (top), [Sr/Fe] (middle), and [Ba/Fe] (bottom) abundances for our four UMP stars (green circles) and the sample of Yong et al. (2013; black crosses). Upper limits are indicated by arrows; the dashed line is the solar value.

(A color version of this figure is available in the online journal.)

studies, such as Sivarani et al. (2006) and Norris et al. (2013b), have found a correlation of [N/Fe] with [C/Fe] for CEMP stars. The N abundance and upper limits that we derive support this correlation. Oxygen was not detected in any of our program stars, and the noise levels in the spectra were too high to compute a meaningful upper limit on its abundance.

3.2.3. Light Elements and Neutron-capture Elements

Since the stars in this sample have been analyzed in a similar manner as those of Yong et al. (2013), the two samples are directly comparable. In the top panel of Figure 5, the mean [α/Fe] (taken to be the mean of [Mg/Fe], [Ca/Fe], and [Ti/Fe]) abundance ratios of our four stars is compared to those of Yong et al. (2013). Their sample includes some of the most metal-poor stars known to date (HE 0107−5240: Christlieb et al. 2002; HE 1327−2326: Frebel et al. 2005; and HE 0557−4840: Norris et al. 2007). A small overabundance of the [α/Fe] ratio is seen in the four new stars, consistent with the existing picture of the α-element abundances in metal-poor stars, reflecting the enrichment from core–collapse SNe in the early universe. Norris et al. (2013b) found that 50% of their CEMP stars are more enhanced in the light elements Na, Mg, Al, and Si, compared to other (C-normal) EMP stars with similar stellar parameters. Among our program stars, HE 0233−0343 exhibits higher abundances of these elements relative to the rest of the sample. However, none of our stars show overabundances of these elements as large as those found for some CEMP stars in the sample of Norris et al. (2013b). The observed abundances for Al and Mn in our four stars lie somewhat below the level predicted by the Galactic chemical evolution models of Nomoto et al. (2013). This may be due to NLTE effects. Gehren et al. (2004) report NLTE corrections of +0.5 dex for Al in a sample of metal-poor turn-off stars, while Bergemann & Gehren (2008) find corrections of up to +0.7 dex for Mn in their sample of metal-poor giant and dwarf stars. This would bring Al to the predicted level, whereas Mn would stay just below.

The middle and bottom panels of Figure 5 display the [Sr/Fe] and [Ba/Fe] abundance ratios, respectively, as functions of metallicity for our program stars and those of Yong et al. (2013). Both samples exhibit a large spread in the [Sr/Fe] and [Ba/Fe] ratios. The spread of abundances for these two elements was also discussed by Hansen et al. (2012, 2013) and Yong et al. (2013), all suggesting that more than one production site exists for Sr and Ba. The scatter in the Sr and Ba abundances of EMP stars has also been discussed by Aoki et al. (2013), who studied the [Sr/Ba] ratios in a sample of 260 EMP stars. They detected no stars with [Sr/Fe] > 0.0 for [Fe/H] < -3.6 (note that their sample only includes four stars with [Fe/H] < -3.6). They proposed to explain the distribution in the observed [Sr/Ba] ratios with a truncated *r*-process taking place in a type II SN, as described by Boyd et al. (2012). Aoki et al. (2013) also stated that neither the *r* process nor the truncated *r* process are expected to produce stars with [Sr/Ba] < -0.5. They find six stars in their sample with [Sr/Ba] < -0.5, but suspect these to be contaminated with *s*-process material.

4. DISCUSSION

The lithium abundances in carbon-enhanced stars is a relatively unexplored chapter in the history of Galactic chemical evolution; theoretical efforts include Stancliffe (2009). Only a few CEMP stars have detected lithium and even fewer of these are CEMP-no stars, though the samples of CEMP-no stars are increasing quickly, in particular, from dedicated searches for CEMP stars (e.g., Placco et al. 2010, 2011, 2013, 2014). We have detected Li for two of the stars in our sample and the derived Li abundances for these indicate a Li depletion in the stars relative to the Spite Li plateau. These detections highlight the need for a progenitor of CEMP-no stars that produces large amounts of carbon, but only small amounts of neutron-capture elements, while to some extent depleting the lithium. Masseron et al. (2012) test how mass transfer from an AGB companion will affect the Li abundance of a CEMP star. They examined a set of different AGB models and different depletion factors for the transferred material, but found that none of the models could explain the observed spread in Li abundances of the CEMP-no stars of their sample. The other suggested progenitor candidates for the CEMP-no stars include faint SNe that experienced mixing and fallback, as well as spinstars. If these are indeed the progenitors, the Li abundance of CEMP-no stars should lie below the level found in non-carbon-enhanced stars, as Li should be depleted (or totally destroyed) in such objects. Hence, when the gas from these mixes with the ISM in their surroundings (and forms the CEMP-no stars), the overall Li abundance will be lowered (Meynet et al. 2010). In fact, as suggested by Piau et al. (2006), this process might be responsible for the lowering of the primordial Li abundance from the level predicted from big bang nucleosynthesis calculations, the lack of scatter among stars on the plateau at metallicities $-2.5 <$ [Fe/H] < -1.5, due to complete mixing (e.g., Ryan et al. 1999), the downturn and increase of scatter in the Li abundances for stars with [Fe/H] < -2.5, due to incomplete local mixing (Sbordone et al. 2010), and the very low (or absent) Li among the lowest metallicity stars (e.g., Frebel et al. 2005; Keller et al. 2014).

The sample of Li measurements for CEMP-no stars is presently very limited, and at this stage all of the proposed

progenitors of CEMP-no stars involve some variation of mixing. When mixing has occurred, it is natural that the Li abundance is depleted, leading to lower abundances of lithium in carbon-enhanced stars. Also, it is uncertain how much of the Li can be depleted after a possible mass transfer via mixing and rotation of the CEMP star itself (Talon & Charbonnel 2005; Stancliffe et al. 2007). More Li detections (or strong upper limits) in CEMP-no stars are needed in order to better understand the nature of the progenitors of these stars.

The carbon enhancement, detected for three of our four program stars is consistent with the picture of carbon enhancement in the early universe found by other authors (e.g., Carollo et al. 2012; Norris et al. 2013b). An enrichment of carbon in the early universe also supports one of the proposed formation scenarios for low-mass stars, that gas clouds can fragment as a result of cooling via fine-structure lines of carbon and oxygen (Frebel et al. 2007).

Spite et al. (2013) examined the carbon abundances of dwarfs and turnoff stars, stars in which mixing has not altered the carbon abundance at the surface of the star. From their sample, they suggested the presence of two plateaus of the carbon abundances, one for [Fe/H] > -3.0 at $A(\mathrm{C}) \sim 8.25$ and one for [Fe/H] < -3.4 at $A(\mathrm{C}) \sim 6.8$. They point to the low number of stars observed with [Fe/H] < -3.4, and highlight the difficulty of observing carbon in warmer, unmixed stars. As a result, they could not conclude if the lower plateau is just an upper limit on the detections or an actual plateau. We derive a carbon abundance of $A(\mathrm{C}) = 7.23$ for the unmixed CEMP subgiant in our sample HE 0233−0343, placing it a little above the plateau. Clearly, observations of additional unmixed CEMP stars are needed to clarify if such a plateau exists.

The origin of neutron-capture elements in low-metallicity stars is not yet well understood. A large spread is seen in the abundances of the neutron-capture elements Sr and Ba for CEMP-no stars (indistinguishable from that of non-carbon-rich metal-poor stars). For the CEMP-*s* stars, the carbon and *s*-process overabundances are believed to be the result of mass transfer from a binary AGB companion. Indeed, Lucatello et al. (2005) showed that a significant fraction of these stars (perhaps all) are in fact in binary systems. For the CEMP-no stars, however, early results from radial-velocity monitoring do not require them to be in binary systems (Cohen et al. 2013; Hansen et al. 2013; Norris et al. 2013b; Starkenburg et al. 2014; J. Andersen et al., in preparation).

Figure 6 shows the derived [Sr/Ba] ratios of our three CEMP-no stars, together with the ratios for stars from the Yong et al. (2013) sample that had detections of both Sr and Ba. The dashed red line indicates [Sr/Ba] $= -0.4$, used as an upper limit for the main *s*-process signature of AGB stars (Spite et al. 2013). At solar metallicity, Sr is a tracer of the weak *s* process, in massive stars (Heil et al. 2009; Pignatari et al. 2010), while Ba is a tracer of the main *s* process taking place in AGB stars (Busso et al. 1999; Käppeler et al. 2011). At low metallicity, where the main *s* process is not yet active, the picture is different.

To assess the origin of the Sr and Ba detected for our three CEMP-no stars, the [Sr/Ba] ratio can be compared to that for classical main *s*-process-enhanced metal-poor stars, and in strongly *r*-process-enhanced metal-poor stars. Lucatello et al. (2003) reported on the abundances analysis of HE 0024−2523, a classical main *s*-process-enhanced star with carbon enhancement. This star was also found to be in a binary system, and the authors argued that the carbon and *s*-process element enhancement is the result of mass transfer from an AGB

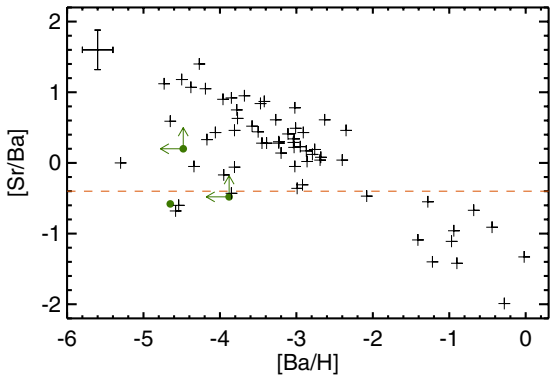

Figure 6. [Sr/Ba] ratios plotted against Ba abundances, [Ba/H], for our three CEMP-no stars (green circles) and the sample of Yong et al. (2013; black crosses). Arrows indicate upper limits; the dashed red line indicates [Sr/Ba] $= -0.4$. Ratios above this line indicate production of Sr and Ba by the weak *s* process in massive stars or by the *r* process, while those below indicate production by the main *s* process in AGB stars.

(A color version of this figure is available in the online journal.)

companion. The [Sr/Ba] ratio in this star is [Sr/Ba] $= -1.12$, a very low value, due to its high Ba abundance. Although a large spread is seen in the efficiency of the main *s*-process element production of the AGB stars (Bisterzo et al. 2011), a low [Sr/Ba] ratio is observed for *s*-process elements produced in AGB stars; Spite et al. (2013) use [Sr/Ba] < -0.4 as an upper limit, while [Sr/Ba] $= -0.5$ was used by Aoki et al. (2013). For our CEMP-no stars, we find the following [Sr/Ba] ratios: [Sr/Ba] $> +0.20$ (HE 0134−1519), [Sr/Ba] > -0.48 (HE 0233−0343), and [Sr/Ba] $= -0.58$ (HE 1310−0536). The ratios found in HE 0233−0343 and HE 1310−0536 could indicate production by the main *s* process. However, these stars are CEMP-no stars, i.e., their individual abundance ratios of Ba relative to iron are low ([Ba/Fe] < 0), and they are also UMP stars ([Fe/H] < -4.0). At such low metallicity, the Ba is more likely produced in the main *r* process from SNe and Sr in the weak *s* process in massive stars. The following [Sr/Ba] ratios have been found in strongly *r*-process-enhanced metal-poor stars, [Sr/Ba] $= -0.52$ in CS 31082-001 (Hill et al. 2002), [Sr/Ba] $= -0.41$ for CS 22892-052 (Sneden et al. 2003), and [Sr/Ba] $= -0.46$ for CS 29497-004 (Christlieb et al. 2004). These ratios are, very similar to those we find, for HE 0233−0343 and HE 1310−0536. The [Sr/Ba] ratio found for HE 0134−1519 indicates that the Sr and Ba in this star could have been produced in the weak *s*-process in spinstars.

Cescutti et al. (2013) proposed that the spread in Sr and Ba abundances detected in CEMP-no stars could be explained by spinstar progenitors. Their model includes a standard *r* process (presumably in the natal clouds) plus a contribution from the weak *s* process occurring in spinstars. With this combination, they can model the spread seen in the abundances of Sr and Ba in metal-poor stars, including the CEMP-no stars, while also reproducing the low scatter in α elements. They do, however, state that their models cannot reproduce the [C/O] and [N/O] ratios in the same CEMP-no stars, but point to the scenario of Meynet et al. (2010), where low-mass stars belonging to the forming stellar cluster of a spinstar are enriched in carbon via stellar winds from the spinstar.

5. SUMMARY

We have conducted a detailed chemical-abundance analysis of four new UMP stars, with [Fe/H] $\leqslant -4.0$; fewer than

10 such stars were previously known. The Li, C, Sr, and Ba measurements provide a new observational window to examine nucleosynthesis at the earliest times in our Galaxy. While one star has an upper limit of [C/Fe] $< +1.7$, the remaining three stars are all C-rich, confirming the prevalence of CEMP stars in the early universe. The detection of Li in two of the clear CEMP-no stars requires that whatever process(es) produce(s) the large amount of C (and presumably the N, O often found in CEMP-no stars, but which could not be detected in our stars), does not completely destroy Li. In light of the newer data for C and Li for these, and other recently studied CEMP-no stars, we suggest that it is worth revisiting the Li astration model described by Piau et al. (2006). Finally, our detections of Sr and Ba for several additional UMP stars demonstrates that the process(es) creating these elements are at work even at very low metallicities, a conclusion also reached by Roederer (2013). Since there still remain a number of stars at the lowest metallicities with only upper limits on Sr and/or Ba, increasing the sample sizes and the quality of the available high-resolution spectroscopy for stars at these metallicities is an essential step toward understanding nucleosynthesis at the earliest epochs and ultimately to characterize "the frequency and environmental influence of the astrophysical sites of heavy-element production" (Roederer 2013).

We thank E. Caffau for providing the spectrum of SDSS J102915+172927. This work was supported by Sonderforschungsbereich SFB 881 "The Milky Way System" (subproject A4) of the German Research Foundation (DFG). T.C.B. acknowledges partial support from grant PHY 08-22648: Physics Frontier Center/Joint Institute for Nuclear Astrophysics (JINA), awarded by the U.S. National Science Foundation. V.M.P. acknowledges support from the Gemini Observatory. M.A., M.S.B., J.E.N., and D.Y. acknowledge support from the Australian Research Council (grants DP0342613, DP0663562, and FL110100012) for studies of the Galaxy's most metal-poor stars. A.F. acknowledges support from NSF grant AST-1255160. Furthermore, we thank the referee for helpful comments.

This work made use of the Southern Astrophysical Research (SOAR) 4.1 m Telescope (proposal SO2013B-001), which is a joint project of the Ministério da Ciência, Tecnologia, e Inovação (MCTI) da República Federativa do Brasil, the U.S. National Optical Astronomy Observatory (NOAO), the University of North Carolina at Chapel Hill (UNC), and Michigan State University (MSU).

This work also made use of the Kitt Peak National Observatory Mayall 4 m Telescope (proposal 2013B-0046) of the National Optical Astronomy Observatory, which is operated by the Association of American Universities for Research in Astronomy (AURA), under cooperative agreement with the National Science Foundation.

This work also made use of observations conducted with ESO Telescopes at the La Silla Observatory and the VLT on Paranal, under programme ID 69.D-0130(A).

REFERENCES

Allende Prieto, C., Barklem, P. S., Lambert, D. L., & Cunha, K. 2004, A&A, 420, 183
Aoki, W. 2010, in IAU Symp. 265, Chemical Abundances in the Universe: Connecting First Stars to Planets, ed. K. Cunba, M. Spite, & B. Barbuy (Cambridge: Cambridge Univ. Press), 111
Aoki, W., Beers, T. C., Christlieb, N., et al. 2007, ApJ, 655, 492
Aoki, W., Suda, T., Boyd, R. N., Kajino, T., & Famiano, M. A. 2013, ApJL, 766, L13
Asplund, M., Grevesse, N., Sauval, A. J., & Scott, P. 2009, ARA&A, 47, 481
Asplund, M., Lambert, D. L., Nissen, P. E., Primas, F., & Smith, V. V. 2006, ApJ, 644, 229
Beers, T. C., Carollo, D., Ivezic, Z., et al. 2012, ApJ, 746, 34
Beers, T. C., & Christlieb, N. 2005, ARA&A, 43, 531
Beers, T. C., Flynn, C., Rossi, S., et al. 2007, ApJS, 168, 128
Bergemann, M., & Gehren, T. 2008, A&A, 492, 823
Bergemann, M., Lind, K., Collet, R., Magic, Z., & Asplund, M. 2012, MNRAS, 427, 27
Bessell, M. S. 2007, PASP, 119, 605
Bisterzo, S., Gallino, R., Straniero, O., Cristallo, S., & Käppeler, F. 2011, MNRAS, 422, 849
Boyd, R. N., Famiano, M. A., Meyer, B. S., et al. 2012, ApJL, 744, L14
Burbidge, E. M., Burbidge, G. R., Fowler, W. A., & Hoyle, F. 1957, RvMP, 29, 547
Busso, M., Gallino, R., & Wasserburg, G. J. 1999, ARA&A, 37, 239
Caffau, E., Bonifacio, P., François, P., et al. 2011, Natur, 477, 67
Carollo, D., Beers, T. C., Bovy, J., et al. 2012, ApJ, 744, 195
Carollo, D., Beers, T. C., Chiba, M., et al. 2010, ApJ, 712, 692
Carollo, D., Beers, T. C., Lee, Y. S., et al. 2007, Natur, 450, 1020
Carollo, D., Freeman, K. C., Beers, T. C., et al. 2014, ApJ, submitted (arXiv:1401.0574)
Castelli, F., & Kurucz, R. L. 2003, in IAU Symp. 210, Modelling of Stellar Atmospheres, ed. N. Piskunov, W. W. Weiss, & D. F. Gray (San Francisco, CA: ASP), 20
Cayrel, R., Depagne, E., Spite, M., et al. 2004, A&A, 416, 1117
Cescutti, G., Chiappini, C., Hirschi, R., Meynet, G., & Frischknecht, U. 2013, A&A, 553, A51
Christlieb, N., Beers, T. C., Barklmen, P. S., et al. 2004, A&A, 428, 1027
Christlieb, N., Bessell, M. S., Beers, T. C., et al. 2002, Natur, 419, 904
Cohen, J. G., Christlieb, N., Thompson, I., et al. 2013, ApJ, 778, 56
Collet, R., Asplund, M., & Trampedach, R. 2006, ApJL, 644, L121
Dekker, H., D'Odorico, S., Kaufer, A., Delabra, B., & Kotzlowski, H. 2000, Proc. SPIE, 4008, 534
Demarque, P., Woo, J. H., Kim, Y. C., & Yi, S. K. 2004, ApJS, 155, 667
Dopita, M., Hart, J., McGregor, P., et al. 2007, Ap&SS, 310, 255
Frebel, A., Aoki, W., Christlieb, N., et al. 2005, Natur, 434, 871
Frebel, A., Johnson, J. L., & Bromm, V. 2007, MNRAS, 380, L40
Gehren, T., Liang, Y. C., Shi, J. R., et al. 2004, A&A, 413, 1045
Gustafsson, B., Edvardsson, B., Eriksson, K., et al. 2008, A&A, 486, 951
Hansen, C. J., Bergemann, M., & Cescutti, G. 2013, A&A, 551, A57
Hansen, C. J., Primas, F., & Hartman, H. 2012, A&A, 545, A31
Hansen, T., Andersen, J., & Nordström, B. 2013, Proceedings of Science (NIC XII), Heavy Elements in the Early Galaxy, ed. J. Lattanzio, A. Karakas, M. Lugaro, & G. Dracoulis (published online at http://pos.sissa.it/cgi-bin/reader/conf.cgi?confid=146)
Hansen, T., Andersen, J., Nordström, B., Buchhave, L. A., & Beers, T. C. 2011, ApJL, 743, L1
Heil, M., Juseviciute, A., Käppeler, F., et al. 2009, PASA, 26, 243
Herwig, F. 2005, ARA&A, 43, 435
Hill, V., Plez, B., Cayrel, R., et al. 2002, A&A, 387, 560
Hirschi, R. 2007, A&A, 461, 571
Hirschi, R., Frölich, C., Liebendörfer, M., & Thieleman, F.-K. 2006, RvMA, 19, 101
Ito, H., Aoki, W., Beers, T. C., et al. 2013, ApJ, 773, 33
Ito, H., Aoki, W., Honda, S., & Beers, T. C. 2009, ApJL, 698, L37
Käppeler, F., Gallino, R., Bisterzo, S., & Aoki, W. 2011, RvMP, 83, 157
Keller, S. C., Bessel, M. S., Frebel, A., et al. 2014, Natur, 506, 463
Kupka, F. G., Ryabchikova, T. A., Piskunov, N. E., Stempels, H. C., & Weiss, W. W. 2000, BaltA, 9, 590
Kurucz, R. L. 1995, in ASP Conf. Ser. 78, Astrophysical Applications of Powerful New Databases, ed. S. J. Adelman & W. L. Wiese (San Francisco, CA: ASP), 78
Lee, Y. S., Beers, T. C., Masseron, T., et al. 2013, AJ, 146, 132
Lind, K., Bergemann, M., & Asplund, M. 2012, MNRAS, 427, 50
Lucatello, S., Gratton, R., Cohen, J. C., et al. 2003, ApJ, 125, 875
Lucatello, S., Tsangarides, S., Beers, T. C., et al. 2005, ApJ, 625, 825
Masseron, T., Johnson, J. A., Lucatello, S., et al. 2012, ApJ, 751, 14
Masseron, T., Johnson, J. A., Plez, B., et al. 2010, A&A, 509, A93
McWilliam, A. 1998, AJ, 115, 1640
Meynet, G., Ekström, S., & Maeder, A. 2006, A&A, 447, 623
Meynet, G., Hirschi, R., Ekström, S., et al. 2010, A&A, 521, A30
Nomoto, K., Kobayashi, C., & Tominaga, N. 2013, ARA&A, 51, 457
Norris, J. E., Bessell, M. S., Yong, D., et al. 2013a, ApJ, 762, 25
Norris, J. E., Christlieb, N., Korn, A. J., et al. 2007, ApJ, 670, 774
Norris, J. E., Yong, D., Bessell, M. S., et al. 2013b, ApJ, 762, 28
Piau, L., Beers, T. C., Balsara, D. S., et al. 2006, ApJ, 653, 300

Pignatari, M., Gallino, R., Heil, M., et al. 2010, ApJ, 710, 1557
Pignatari, M., Gallino, R., Meynet, G., et al. 2008, ApJL, 687, L95
Placco, V. M., Frebel, A., Beers, T. C., et al. 2013, ApJ, 770, 104
Placco, V. M., Frebel, A., Beers, T. C., et al. 2014, ApJ, 781, 40
Placco, V. M., Kennedy, C. R., Beers, T. C., et al. 2011, AJ, 142, 188
Placco, V. M., Kennedy, C. R., Rossi, S., et al. 2010, AJ, 139, 1051
Reddy, B. E., Tomkin, J., Lambert, D. L., & Allende Prieto, C. 2003, MNRAS, 340, 304
Roederer, I. U. 2013, AJ, 145, 26
Ryan, S. G., Norris, J. E., & Beers, T. C. 1999, ApJ, 523, 654
Sackmann, I. J., & Boothroyd, A. I. 1992, ApJL, 392, L71
Sbordone, L., Bonifacio, P., Caffau, E., et al. 2010, A&A, 522, A26
Sivarani, T., Beers, T. C., Bonifacio, P., et al. 2006, A&A, 459, 125
Sneden, C. 1973, ApJ, 184, 839
Sneden, C., Cowan, J. J., & Gallino, R. 2008, ARA&A, 46, 241
Sneden, C., Cowan, J. J., Lawler, J. E., et al. 2003, ApJ, 591, 936
Sobeck, J. S., Kraft, R. P., Sneden, C., et al. 2011, AJ, 141, 175
Spite, F., & Spite, M. 1982, A&A, 115, 357
Spite, M., Caffau, E., Bonifacio, P., et al. 2013, A&A, 552, A107
Stancliffe, R. J. 2009, MNRAS, 394, 1051
Stancliffe, R. J., Glebbeek, E., Izzard, R. G., & Pols, O. R. 2007, A&A, 464, L57
Starkenburg, E., Shetrone, M., McConnachie, A., & Venn, K. 2014, MNRAS, in press
Suda, T., Aikawa, M., Machida, M. N., Jujimoto, M. Y., & Iben, I., Jr. 2004, ApJ, 611, 476
Talon, S., & Charbonnel, C. 2005, A&A, 440, 981
Thielemann, F. K., Arcones, A., Käppeli, R., et al. 2011, PrPNP, 66, 346
Tominaga, N., Iwamoto, N., & Nomoto, K. 2013, ApJ, 785, 98
Tominaga, N., Umeda, H., & Nomoto, K. 2007, ApJ, 660, 516
Truran, J. W. 1981, A&A, 97, 391
Umeda, H., & Nomoto, K. 2003, Natur, 422, 871
Umeda, H., & Nomoto, K. 2005, ApJ, 619, 427
Yong, D., Norris, J. E., Bessell, M. S., et al. 2013, ApJ, 762, 26